Human Pathology (2019) **89**, 51–61

ELSEVIER

Human PATHOLOGY

www.elsevier.com/locate/humpath

Original contribution

Childhood pulmonary Langerhans cell histiocytosis: a comprehensive clinical-histopathological and *BRAF*^{V600E} mutation study from the French national cohort☆

Marianne Kambouchner MD[a,*], Jean-François Emile MD, PhD[b], Marie-Christine Copin MD[c], Aurore Coulomb-Lherminé MD, PhD[d], Jean-Christophe Sabourin MD, PhD[e], Valeria Della Valle MD[f], Chiara Sileo MD[f], Hubert Ducou Le Pointe MD, PhD[f], Hugues Bégueret MD[g], Louise Galmiche MD[h], Anne Lambilliotte MD[i], François Paraf MD[j], Marjorie Piche MD[k], Christophe Piguet MD[l], Anne Rullier MD[m], Véronique Secq MD[n], Isabelle Serre MD[o], Jean-François Bernaudin MD, PhD[p], Jean Donadieu MD[q]

[a]*Pathology Department, APHP, Centre Hospitalier Universitaire (CHU) Avicenne, 93000 Bobigny, France*
[b]*Pathology Department, APHP, CHU Ambroise-Paré, 92104 Boulogne-Billancourt, France*
[c]*Pathology Department, CHU de Lille, 59037 Lille, France*
[d]*Pathology Department, APHP, CHU Armand-Trousseau, 75012 Paris, France*
[e]*Pathology Department, CHU Charles-Nicolle, 76031 Rouen, France*
[f]*Radiology Department, APHP, CHU Armand-Trousseau, 75012 Paris, France*
[g]*Pathology Department, CHU de Bordeaux Haut-Lévêque, 33600 Pessac, France*
[h]*Pathology Department, APHP, CHU Necker–Enfants Malades, 75015 Paris, France*
[i]*Pediatric Hemato-Oncology Department, CHU Jeanne-de-Flandre, 59120 Lille, France*
[j]*Pathology Department, CHU Dupuytren, 87000 Limoges, France*
[k]*Pathology Department, CHU L'Archet, 06202 Nice, France*
[l]*Pediatric Hemato-Oncology, CHU Dupuytren, 87000 Limoges, France*
[m]*Pathology Department, CHU de Bordeaux Pellegrin, 33000 Bordeaux, France*
[n]*Pathology Department, CHU La Timone, 13385 Marseille, France*
[o]*Pathology Department, CHU Gui-de-Chauliac, 34295 Montpellier, France*
[p]*INSERM UMR 1272, UFR SMBH Paris 13 University, 93000 Bobigny, France*
[q]*Pediatric Hemato-Oncology Department and French Referent Centre for Histiocytoses, APHP, CHU Armand-Trousseau, 75012 Paris, France*

Received 4 February 2019; revised 24 April 2019; accepted 25 April 2019

☆ The authors declare no conflicts of interest for this study.

* Corresponding author at: Département d'Anatomie Pathologique, Hôpital Avicenne, 125, route de Stalingrad, 93009Cedex Bobigny, France.
E-mail address: marianne.kambouchner@aphp.fr (M. Kambouchner).

https://doi.org/10.1016/j.humpath.2019.04.005

Keywords:
Pulmonary Langerhans cell histiocytosis;
Childhood;
BRAF^{V600E};
Interstitial lung disease;
Histopathology

Summary Childhood pulmonary Langerhans cell histiocytosis (PLCH) is a rare disease. Its pulmonary histopathology, according to comprehensive clinical-radiological findings and *BRAF*^{V600E} mutation status, has not yet been thoroughly documented. From the 167 childhood PLCH cases entered in the French National Histiocytosis Registry (1983-2016), we retrieved lung biopsies from a consecutive retrospective series of 17 patients, diagnosed when they were 2 weeks to 16 years old (median, 9.4 years), and report the clinical and histopathological findings herein. Histological analyses of biopsies (16 surgical and 1 postmortem) found the following features, alone or associated: Langerhans cell (LC) nodules with cavitation (9/17), cysts (14/17), fibrotic scars (2/17), peribronchiolar topographic distribution of the lesions (10/17), and accessory changes, like stretch emphysema (7/17). Those characteristics closely resemble those describing adult PLCH. However, unusual findings observed were 2 large nodules and a diffuse interstitial LC infiltrate. *BRAF*^{V600E} mutation was detected in 4 of 12 samples tested, notably in the 3 with unusual features. In conclusion, childhood PLCH mostly shares the common histology features already described in adult PLCH, regardless of age. Because smoking is considered the major trigger in PLCH pathogenesis, the findings based on this series suggest other inducers of bronchiolar LC recruitment, especially in very young patients.

1. Introduction

Langerhans cell histiocytosis (LCH), characterized by inflammatory lesions mainly composed of CD1a$^+$ Langerhans cells (CD1a$^+$ LCs), occurs in children and adults [1]. Its having been shown to be associated with somatic mutations, especially *BRAF*^{V600E} (v-*RAF* murine sarcoma viral oncogene homolog B) in ~50% of children [2] and 35% of adults, favors a clonal origin [3]. The lung is frequently the only organ involved in adult pulmonary LCH (PLCH), which is strongly associated with tobacco smoking, considered to be the trigger for CD1a$^+$-LC recruitment in distal airways [4,5].

Unlike adults, childhood PLCH, albeit less frequent, is more commonly associated with extrapulmonary involvement [6], so it can be definitively diagnosed with a broader panel of non-invasive biopsies. Consequently, clinical-histopathological studies on childhood PLCH are scarce and rarely focused on its histopathology [7,8], compared to numerous investigations on large adult series [7,9-11].

This context led us to conduct this retrospective histopathology study on all the childhood PLCHs with available lung tissue specimens entered into the French National Histiocytosis Registry (FNHR) over 34 years (1983-2016) [12]. With access to this unique retrospective cohort, we aimed to describe childhood PLCH histopathology according to clinical and radiological features, and *BRAF*^{V600E} mutation status, when available.

2. Materials and methods

2.1. The FNHR and collection of lung histological material

This study included French patients <18 years old diagnosed with PLCH. To be included in the FNHR, patients had to meet LCH diagnostic criteria and their parents provided informed consent. The FNHR has been authorized by French oversight authorities (CCTIRS, Committee for the Treatment of Health-Related Information no. 09 6191; and CNIL, National Committee for Informatics and Freedoms no. 909027) and recognized as a National Registry by French health authorities since 2008, and its completeness has been verified against multiple separate sources, as required [12].

According to guidelines [13], childhood PLCH was diagnosed based on characteristic computed-tomography (CT) scan abnormalities, confirmed by histology of an extrapulmonary or lung biopsy. In addition to lung involvement, patients were classified according to the number of organs involved, especially any of the 3 defined risk organs (ROs) associated with mortality (liver, spleen or blood) [14]: RO$^-$ (lung involvement alone or with another non-RO affected) or RO$^+$ ($\geq$1 RO involved). Overall disease activity was scored with the Disease Activity Score [15].

For this study, the records of 1844 LCH patients ≤18 years old, diagnosed from January 1983 to December 2016, were retrieved from the FNHR. PLCH was diagnosed in 167 (9.1%) patients and a lung biopsy had been obtained from 20. Among them, 17 specimens (16 surgical lung biopsies, 10 during pneumothorax- curative interventions and 6 for isolated pulmonary abnormalities, and 1 postmortem sample) could be retrieved (paraffin-embedded tissue or slides with stained sections) from 10 pathology departments. For the remaining 3 patients, pathology samples were no longer available and the pathology reports in the charts were too brief to be informative. Routine lung sections were independently reviewed by 2 LCH-experienced pathologists (M.K. and J.-F.B.), blinded to clinical information.

The overall characteristics of the 17 biopsy-cohort patients and the 147 no-lung-biopsy group were compared, particularly the numbers of involved extrapulmonary organs, especially any of the 3 ROs. All patients were followed up until

December 31, 2018 and their therapeutic regimens and outcomes were collected.

2.2. CT scans

Radiological data were available for 16 patients: 6 CT-scan reports, and 10 CT scans reviewed by 3 specialized pediatric radiologists (V.D.V., C.S. and H.D.L.P.) and scored as recommended [16]. The presence/absence of nodules, cysts, costophrenic-angle involvement, alveolar condensation and diffuse ground-glass opacities were systematically recorded. A complete radiological description of this childhood PLCH series has been submitted elsewhere.

2.3. Histological analyses

Hematoxylin-eosin–stained and anti-CD1a–immunolabeled slides were available for the 17 samples. When possible, to better identify remnants of bronchiolar structures, additional sections were immunolabeled for cytokeratin and caldesmon. Section areas were size rated: <1, 1-3 or >3 cm^2. The 17 biopsies were assessed for the following features: LC nodular aggregates, alveolar and interstitial LC infiltrates, cysts, fibrotic scars, topographic distribution and accessory changes, including stretch emphysema and smoking-related changes in the surrounding tissues.

2.4. Detection of the genomic *BRAF*^{V600E} mutation

After histological review and enrichment by macrodissection to ≥10% histiocytes, DNA was extracted from formalin-fixed, paraffin-embedded samples [2], all obtained before any therapy. *BRAF*^{V600E} was detected by pyrosequencing with PyroMark Q24 (Qiagen, Hilden, Germany) for 9, or real-time polymerase chain reaction (PCR; LightCycler 480; Roche, Rotkreuz, Switzerland) for 3. For the patient whose histiocyte component was <10%, a droplet digital PCR assay with a Raindrop system (Raindance Technologies, Lexington, MA) was used [2].

2.5. Statistical analyses

Characteristics of biopsy-cohort patients versus the no-lung-biopsy group were compared. All statistical analyses were computed with Stata v13 software (College Station, TX). Categorical parameters were compared with Fisher's exact test, and quantitative variables were compared with the Mann-Whitney *U* test. All tests were 2-tailed, with $P < .05$ defining significance.

Table 1 Demographic and clinical parameters of childhood PLCH: 17 from the biopsy-cohort vs 147 with no lung biopsy

Characteristics	Biopsy	No lung biopsy	P[a]
Male/female, n	11/6	82/65	NS
Age at diagnosis, years			
LCH (median)	9.5	1.2	0.01
PLCH (median)	10.8	1.4	0.0109
>10 years, n (%)	8 (47%)	22 (15%)	0.004
No. of organs involved at maximal extent (median)	3	5	0.0005
Follow-up, years	13.3	8.5	NS
Disease activity score [15] median of the maximum	6.5	4.2	0.02
Extrapulmonary involvement, n (%)			
RO^+ (liver, blood, spleen) patients	4 (23%)	77 (53%)	0.03
Hematological dysfunction	2 (12%)	58 (40%)	0.032
Liver	3 (18%)	67 (46%)	0.04
Spleen	1 (6%)	56 (38.1%)	0.007
Bone	2 (12%)	110 (75%)	<0.001
Skin	6 (35%)	100 (68%)	0.01
Pituitary	9(53%)	31 (21%)	0.007
Central nervous system	2 (12%)	18 (12%)	NS
Overt pneumothorax	12 (70%)	20 (13.6%)	<0.001
Any systemic treatments/chemotherapies, n (%)	13 (76%)	137 (93%)	0.0109
Deaths, n (%)	5 (29%)	25 (17%)	NS
BRAF^{V600Eb}	4/12 (33.3%)	22/34 (64%)	NS

Abbreviations: NS, non-significant; PLCH: pulmonary Langerhans cell histiocytosis; RO^+, risk organ-affected, according to the international consensus [14]; *BRAF*, v-RAF murine sarcoma viral oncogene homolog B.

[a] Fisher's exact test for qualitative parameters or Kruskal-Wallis test for quantitative variables.

[b] Ratio: positive *BRAF*^{V600E}/number of tests done.

Table 2 Individual characteristics of the 17 childhood PLH patients from the biopsy-cohort and their corresponding histopathological findings

Patient	Clinical and radiological findings						
	Sex	Age at Lung biopsy	Clinical onset	RO status; extrapulmonary disease	PNO	Active smoker *	CT scan (score) †
1	F	2 wk	2 wk	RO^+ blood & spleen; skin, thymus, bowel	No	No	Not done
2	M	4 wk	3 wk	RO^-; skin	Yes	No	Nod (3), cysts (6), CPA^+
3	F	3 mo	3 mo	RO^+ blood; skin	No	No	Nod, cysts, CPA^+, condensation
4	F	14 mo	14 mo	RO^+ blood; bone, thymus	Yes	No	Nod (0), cysts (20), CPA^+
5	M	2 y	2 y	RO^+ liver, skin, blood	Yes	No	Nod (0), cysts (18), CPA^+, condensation
6	F	4.5 y	4.5 y	RO^-; none	Yes	No	Nod (0), cysts (12), CPA^+
7	M	5 y	5 y	RO^-; none	Yes	No	Nod (6), cysts (10), CPA^+
8	M	10 y	10 y	RO^-; none	No	No	Nod, CPA^+
9	M	11 y	10.5 y	RO^-; pituitary	Yes	No	Nod (1), cysts (6), CPA^+
10	F	13.5 y	12 y	RO^-; pituitary	No	No	Nod (6), cysts (2), CPA^+
11	M	14 y	10.5 y	RO^-; pituitary	Yes	Yes 1 y/1 py	Nod (0), cysts (12)
12	M	15 y	15 y	RO^-; pituitary	Yes	Yes 1.2 y/2 py	Nod, cysts
13	M	16.5 y	14 y	RO^-; pituitary	Yes	Yes 3 y/6 py	Nod (1), cysts (7)
14	M	16.5 y	16.5 y	RO^-; pituitary, bone	No	Yes 1 y/1 py	Cysts
15	F	16.5 y	9.7 y	RO^-; pituitary, thyroid	Yes	Yes 3 y/2 py	Nod (1), cysts (1); ground-glass
16	M	17 y	5.2 y	RO^-; pituitary	Yes	Yes 3 y/6 py	Nod, cysts
17	M	18 y	14 y	RO^+ liver; pituitary	Yes	Yes 4 y/3 py	Nod, cysts

3. Results

3.1. Demographic and clinical data

The overall characteristics of the 17 childhood-PLCH biopsy-cohort patients and the 147 no-lung-biopsy group are reported in Table 1. Biopsy-cohort patients were significantly older at diagnosis, had less multisystemic involvement at maximal disease extension, especially RO^+, bone and skin, and less frequent, but not statistically significant, $BRAF^{V600E}$-positivity. Moreover, they had significantly more frequent pneumothoraces and pituitary involvement.

The individual characteristics of each biopsied patient (11 males and 6 females; median age at PLCH diagnosis: 9.5 years [range, 2 weeks-18 years]) are given in Table 2. Equal numbers were over or under 10 years old. Twelve (71%) were classified as RO^- and 5 (29%) RO^+. At PLCH diagnosis, the 10 patients ≤13.5 years old were not tobacco smokers, while the 7 ≥14 years old were active cigarette smokers at the time of biopsy. The mean smoking duration before the biopsy was 1.9 year (range, 1-4 years) with a mean of 3 pack/years (range, 1-6 pack/years). The pulmonary biopsy immediately followed the first clinical symptoms for the 8 patients ≤10 years, but the mean interval between symptom onset and biopsy was 3.6 (range, 0-11.8) years for the 9 older children. Twelve children experienced pneumothoraces. Median follow-up lasted 13.3 years and 5 patients died of the consequences of the pulmonary involvement: 1 sudden death at diagnosis, 1 graft-vs-host disease complicating lung transplantation [17], 1 with untreatable pneumothorax and 2 of late complications of chronic pulmonary insufficiency. Twelve patients received systemic therapy including prednisolone, vinblastine and/or cladribine.

3.2. CT-scan patterns

Radiological abnormalities seen on the 16 childhood-PLCH CT scans are reported in Table 2. Nodules (with a score from 1 to 6 when available) were observed in 70% of the patients (11/16). Most often 1 to 10 mm in diameter, with irregular borders, nodules were centrolobular, sometimes with central cavitation. Cysts observed in all 16 patients were typically thick- or thin-walled, round or ovoid, measuring up to 2 to 3 cm in diameter. For 6 (no. 2, 4-7, 9) of the 9 patients <12 years old, the mean CT-scan cyst score was 12 (range, 6-20).

Clinical and radiological findings	Pulmonary histological analysis						
Outcome; age at last visit; cause of death	Area (cm^2)	$CD1a^+$ LC lesions	Lesion distribution	Additional findings	Cysts	Stretch emphysema	$BRAF^{V600E}$
D, 2 wk; sudden death	>3	Nodular	PB	LC int-alv	None	No	Yes
A; 5.4 y	1-3	Nodular	Non-assessable	LC int-alv	Mixed	No	No
A; 9 y	>3	Nodular, pseudotumor	Diffuse	LC int-alv	Mixed	No	Yes
D, 16 mo; PNO	<1	Nodular	PB	LC int-alv	Fibrous	No	No
A; 18 y	1-3	Nodular, pseudotumor	Diffuse	None	Mixed	No	Yes
D; post-lung transplant; 5 y	1-3	Nodular	PB	None	None	No	Not available
A; 18 y	1-3	Subpleural cysts	PB	None	Mixed	Yes	No
A; 26 y	1-3	Fibrotic scars, few LCs	PB	None	None	Yes	Not available
A; 24 y	<1	Subpleural cysts	Non-assessable	None	Mixed	Non-assessable	No
A; 19 y	>3	Nodular	PB	None	Cellular	No	No
A; 29 y	<1	Subpleural cysts, few LCs	Non-assessable	None	Fibrous	Yes	No
D, 28 y; Respir-I	1-3	Nodular	PB	None	Fibrous	Yes	Not available
A; 16.2 y	1-3	Nodular, fibrotic scars	PB	LC int-alv	Fibrous	Yes	No
A; 30.3 y	<1	Nodular	Non-assessable	None	Fibrous	No	Not available
A; 27 y	>3	Diffuse interstitial	Diffuse	M-alv	None	No	Yes
D, 28 y; Respir-I	1-3	Nodular, few LCs	PB	M-alv	Cellular	Yes	No
A; 32 y	1-3	Subpleural cysts	PB	M-alv	Fibrous	Yes	No

Abbreviations: RO^+/RO^-, respectively, with or without involvement of extrapulmonary risk organs associated with mortality (liver, spleen or blood); PNO pneumothorax; LCs, Langerhans cells; *BRAF*, v-*RAF* murine sarcoma viral oncogene homolog B; py, pack-years; CT, computed-tomography scan, Nod, nodules, CPA^+, costophrenic angle involvement; A, alive, D, dead, Respir-I, respiratory insufficiency; PB, peribronchiolar; LC int-alv, LCs within interstitial and alveolar compartments far from $CD1a^+$-LC nodules; M-alv, macrophage accumulation in alveolar spaces.
*Active smoker at time of biopsy: duration and n of pack-years.
†The number in () indicates the score [16], when available.

Nodules and cysts located near the costophrenic angles in patients 1 to 10 (63%), all <14 years, represented a pediatric specificity, and alveolar condensation appeared as a new specific feature in patients 3 and 5.

3.3. Histopathology

Large tissue sections (>3 cm^2) were analyzed for 4 patients, small biopsies (<1 cm^2) for 4, and intermediate (1-3 cm^2) specimens for the remaining 9 (Table 2). The main histological findings are summarized in Table 2 and shown in Fig. 1. In all specimens, LCs were identified by their usual elongated nuclei with delicate clefts and inconspicuous nucleoli, and pale eosinophilic cytoplasm of indistinct cell borders. Anti-CD1a immunolabeling confirmed that identify in all the specimens.

3.3.1. LC nodules with cavitation

The main (9/17) observed lesion was $CD1a^+$-LC aggregates admixed with various amounts of lymphocytes or eosinophils, forming more-or-less compact nodules centered around small cavities (Fig. 1A and B). These cell aggregates were separated by normal parenchymal bands (Fig. 1A). This pattern was observed in 9 patients (Table 2). In addition, some small $CD1a^+$-LC clusters were located far from the main nodules (patients 1-4 and 13).

3.3.2. Large nodules

In patients 3 and 5, the lung parenchyma was almost entirely infiltrated by CD1a + LCs forming large nodules, comprised more or less compact infiltrates of $CD1a^+$ LCs mixed with eosinophils, the latter with a small cavitation (patient 5; Fig. 2), or extensive infiltration of air spaces and alveolar walls, with the underlying interstitial network still visible, suggesting recent and massive $CD1a^+$-LC expansion (patient 3; Fig. 3).

3.3.3. Alveolar and interstitial LC infiltrates

An unusual diffuse interstitial infiltrative pattern was observed in patient 15's biopsy. The normal alveolar architecture was well-preserved, and bronchioles looked normal. Alveolar walls were infiltrated by sheets of $CD1a^+$ LCs mixed with rare eosinophils and lymphocytes, adjacent alveoli contained small $CD1a^+$-LC clusters intermixed with $CD1a^-$ macrophages, resulting in a pattern of $CD1a^+$-LC interstitial pneumonitis (Fig. 4).

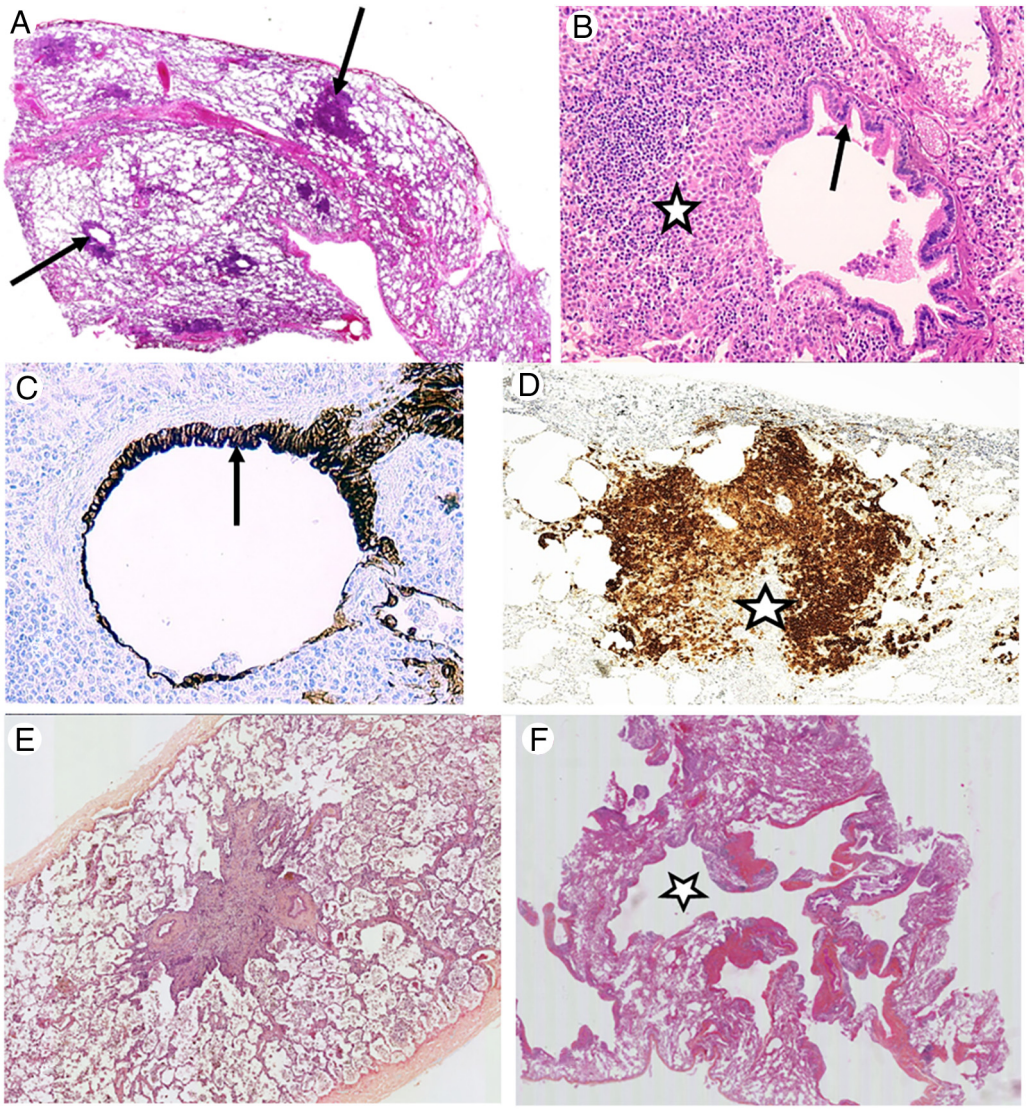

Figure 1 A-C, Patient 10. A, Peribronchiolar Langerhans cell (LC) aggregates with cavitation (arrows). B, Higher magnification shows the characteristic breakdown of the bronchiolar mucosa (arrow) by LC aggregates (star). C, Cytokeratin immunolabeling highlights remnants of bronchiolar lining (arrow) within a bronchiolectasia associated with a LC nodule. D, Patient 6. Subpleural aggregate of immunolabeled CD1a^{+} LCs (star). E, Patient 8. Typical pattern of bronchiolar starfish scar. F, Patient 17. Thick-walled cyst in continuity with a bronchiolar lumen (star). Hematoxylin-eosin staining (A, B, E, and F); original magnifications: ×25 (A, E, and F) or ×50 (B, C, and D).

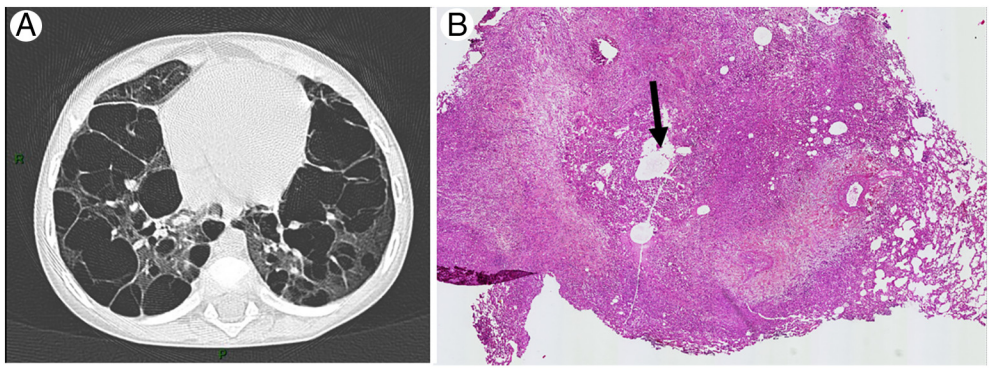

Figure 2 Patient 5, a 2-year-old *BRAF*^{V600E}-positive boy. A, Chest computed tomogram showing extensive cystic changes. B, Overview of the lung biopsy showing more-or-less compact extension of Langerhans cell infiltrates, the latter with a small central cavitation (arrow). Hematoxylin-eosin staining; original magnification ×25.

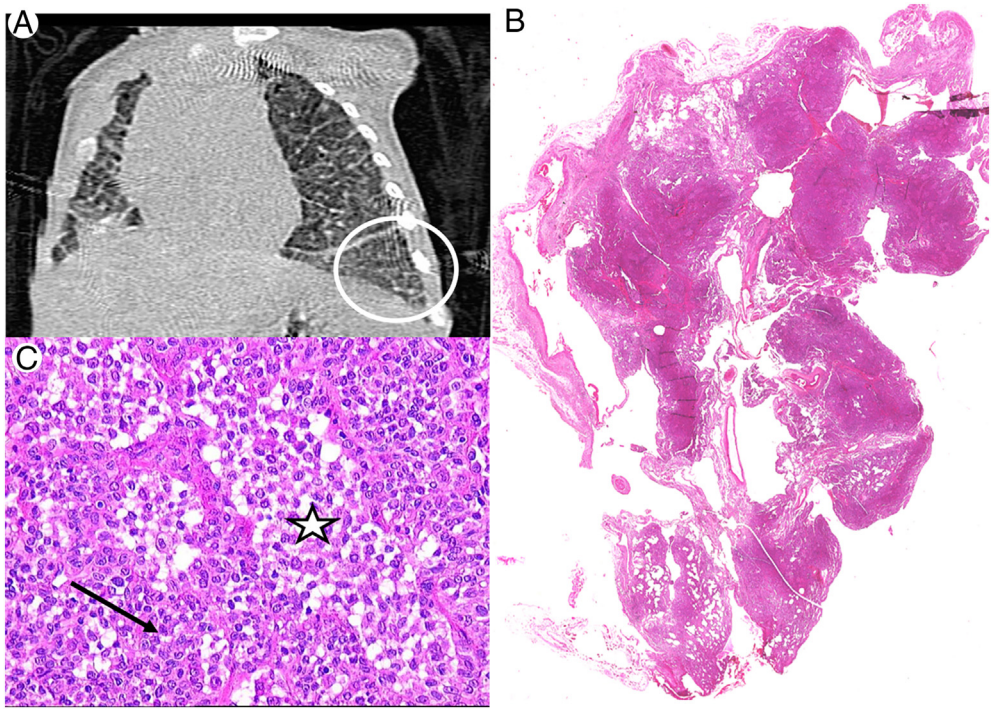

Figure 3 Patient 3. A, Axial chest computed tomogram showing thickened septa and condensation visible in the costophrenic angle (encircled). B, Low magnification of the biopsy showing a coalesced nodular-shaped infiltrate of Langerhans cells (LCs). C, Massive LC infiltration of both airspaces (star) and alveolar walls (arrow). Hematoxylin-eosin staining; original magnification ×25 (B) or ×50 (C).

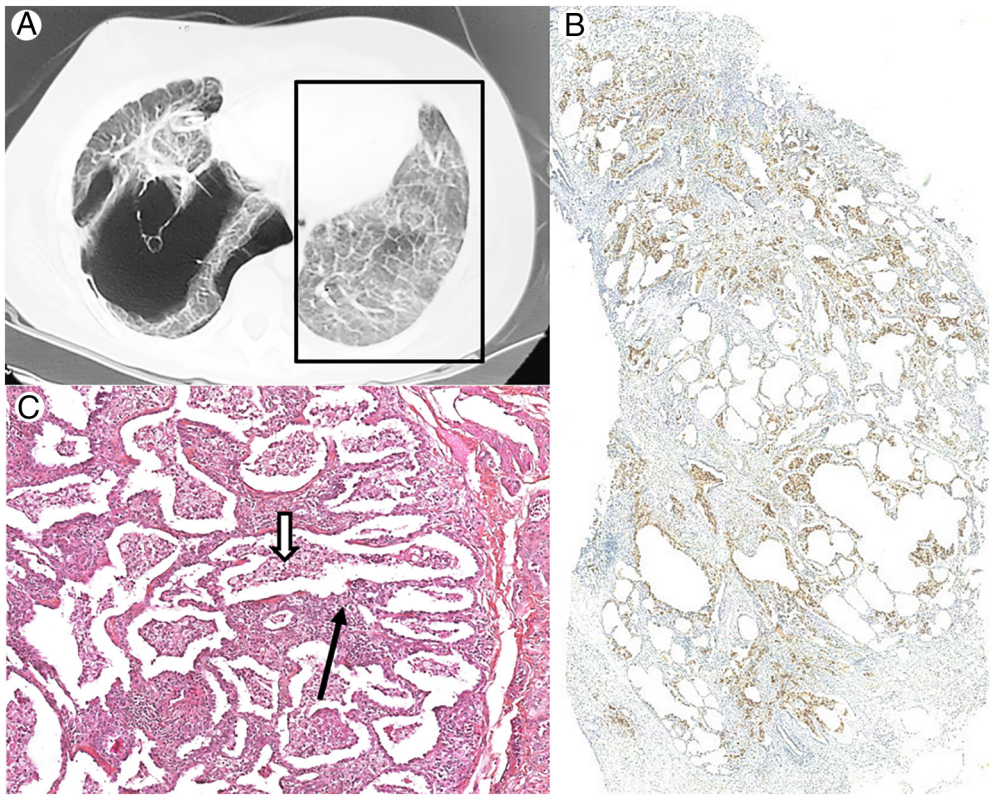

Fig.4 Patient 15: a 16.5-year-old *BRAF*^{V600E}-positive girl, active smoker. A, Chest computed tomogram shows thickening of the septae and diffuse ground-glass opacities (framed in the box). B, Low magnification of CD1a-immunolabeling demonstrating both interstitial and alveolar infiltration of diffuse Langerhans cell (LC) clusters (original magnification ×25). C, Diffuse alveolar (thick arrow) and interstitial (thin arrow) LC infiltration associated with preservation of lung architecture (hematoxylin-eosin staining; original magnification ×100).

3.3.4. Cysts

Cystic remodeling was observed in most of the biopsies (13/17 [76%]). In addition to the usual nodule cavitation observed (Fig. 1A and C; Fig. 2B), a predominant pattern made of subpleural cysts surrounded by CD1a$^+$-LC clusters was observed in patients 7, 9, 11 and 17, notably those whose biopsies had been obtained concurrently with pneumothorax cure (Figs. 1F and 5C). Cyst walls were either fibrous and thin containing rare CD1a$^+$ LCs (5/11; 45%) or cellular with still numerous CD1a$^+$ LCs (6/11; 55%) (Fig. 1F and 5C). Importantly, cysts were seen in infants with no tobacco exposure.

3.3.5. Fibrotic scars

Healing lesions, like the so-called "starfish scars" (Fig. 1E) or fibrous nodules, were seen in biopsies from patients 8 and 13.

3.3.6. Topographic distribution of PLCH lesions

For 7 (41%) patients, the narrowness of their subpleural specimens (<1 cm^2) or the diffuse extension of lesions prevented suitable evaluation of PLCH topographic distribution in relationship to peripheral bronchioles (Table 2). Bronchiolar mucosal remnants were sometimes identified, either on hematoxylin-eosin–stained or anti-cytokeratin– or anti-caldesmon–immunolabeled tissue (Fig. 1C). For 9 patients with sufficiently large areas, CD1a$^+$ LCs predominated in lobule centers, in contact with bronchiolar walls (Fig. 1A-C). That centrolobular LC-lesion topography was even observed in the lungs of very young patients 1 and 4.

3.3.7. Accessory changes

Stretch emphysema was observed in 7 of 17 samples, mostly in apparently older lesions (Table 2).

Histological changes commonly associated with long-term smoking (respiratory bronchiolitis, brown-pigmented macrophage alveolitis) were absent, even when patients 11 to 17 were active tobacco smoker at the time their biopsies were obtained. This finding probably reflects the relatively recent onset of smoking. Also, hemosiderin-laden macrophages were very scarce.

3.4. Histopathology according to CT scan and age

A nodular pattern observed in 9 of 16 (56%) CT scans was also found in 11 of 16 (68%) tissue samples. CT scans showed pulmonary cysts in 15 (94%). However, due to the sampling site, cysts were histologically observed in only 13 of 17 (76%) tissue specimens. Importantly, 5 of the 8 lung biopsies from patients ≤10 years old, including children as young as 4 weeks, contained cysts.

Patients 3, 5 and 15 had unusual histological diffuse infiltrative patterns. Alveolar condensations were seen on the CT scan of patients 3 and 5 who had large nodules. Patient 15's CT scan showed diffuse ground-glass opacities, and her biopsy contained diffuse alveolar and interstitial LC infiltrates evocative of CD1a$^+$-LC interstitial pneumonitis.

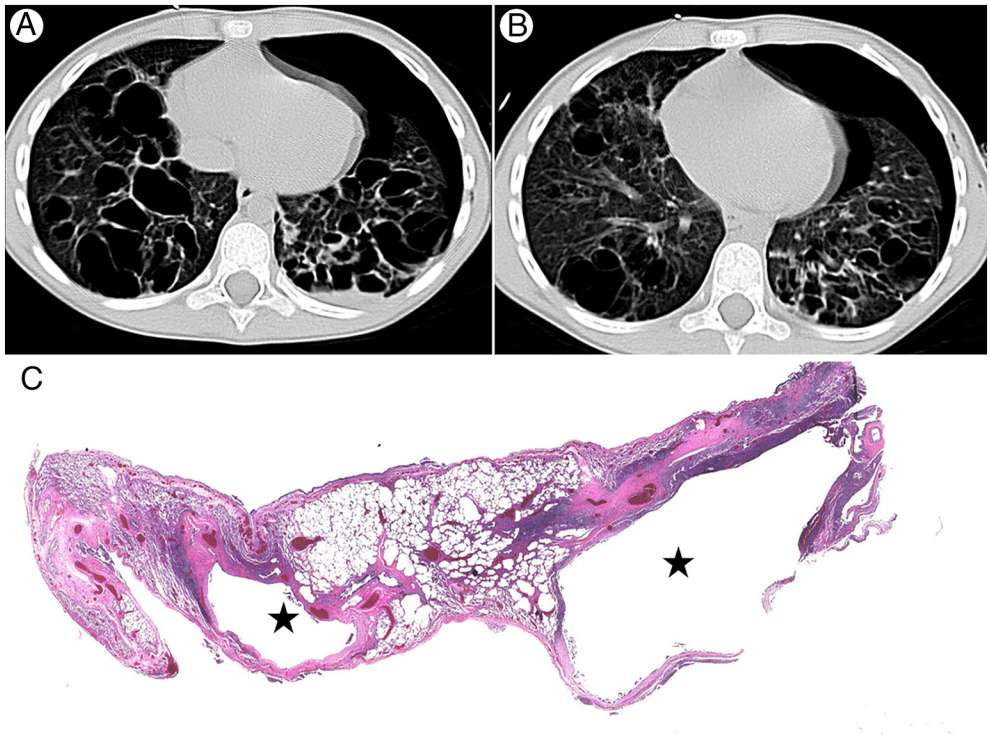

Fig 5 Patient 7: a 5-year-old boy. A and B, Chest computed tomograms showing diffuse, bilateral, thick-walled cysts and left pneumothorax. C, Lung-biopsy histology confirmed cystic spaces (stars) surrounded by mixed cellular and fibrotic Langerhans cell lesions (hematoxylin-eosin staining; original magnification ×25).

3.5. Histopathology according to *BRAF*^{V600E} mutation

Interestingly, the 4 *BRAF*^{V600E} mutation carriers were: newborn patient 1, 3-month-old female patient 3, 2-year-old male patient 5 whose pulmonary biopsies demonstrated massive CD1a$^+$-LC infiltrations, and16.5-year-old female patient 15 who had an unusual diffuse interstitial pneumonitis pattern. Notably, these 4 cases were characterized by the histopathological and radiological absence of typical circumscribed LC nodules and scarcity of cysts.

4. Discussion

In the FNHR cohort, 9.1% of LCH patients ≤18 years old have PLCH. Lung biopsies had been obtained for diagnosis from 12% of the cohort; this low lung-biopsy rate agrees with a previous series [13]. However, that earlier study reported no histopathology findings [13]. Indeed, histopathology reports dealing with childhood PLCH are scarce [7,8], mostly sporadic clinical-pathological cases [18-22], thereby making this analysis of 17 childhood-PLCH biopsies the largest series to be reported [7,8,18-23].

The first issue concerns this series' representativeness of childhood-PLCH histopathology. Actually, most of the 147 no-lung-biopsy group were younger, with more diffuse disease, allowing diagnosis based on non-invasive biopsies. The higher pneumothorax rate in the biopsy cohort might explain the higher likelihood of obtaining a lung biopsy [7,8,18-23]. Nevertheless, our series' biopsies were obtained from children 2 weeks to 18 years old, with RO$^+$ or RO$^-$ extrapulmonary disease extension. Other than these limitations, the histopathology patterns found in this series can be considered representative of childhood PLCH. Similar characteristics were described in the few childhood-PLCH cases published [7,8,18-23] and the largest study so far on 102 children with PLCH, among whom only 12 (12%) underwent lung biopsy [13]. However, it seems important to keep in mind potential bias, with constant underrepresentation of the youngest patients, with less extensive disease.

Technically, the main study limitations were the small sizes of the pediatric pulmonary biopsies (4 cases <1 cm^2) and thinness of the subpleural samples obtained to cure pneumothorax, because they prevented reliable histological analyses to detect the vascular changes described in adults [24] but not yet evaluated in childhood PLCH.

Pertinently, most of the lesions in our biopsied patients shared the same histological pattern as that described in adult PLCH. Indeed, tissue specimens sufficiently large to allow easy interpretation exhibited the archetypal histology of adult PLCH, ie, coexistence of CD1a$^+$-LC aggregates admixed with inflammatory cells, forming nodules in a bronchiolocentric distribution, and variously aged cysts, even in very young children. In addition, as previously described in adults, bronchiolar mucosa was frequently broken in the middle of CD1a$^+$-LC clusters. It must be emphasized that fibrous or mixed-pattern cysts were observed in 4 of the 5 samples from children ≤2 years.

Importantly, cystic changes represent a characteristic histopathologic feature of adult PLCH [7,9-11]. As we previously demonstrated in a 3-dimensional study, the elective location of CD1a$^+$-LC lesions along the bronchiolar axis, undoubtedly indicates the role of the bronchiolar lumen in the pathophysiology of most cystic spaces observed in adult PCLHs [25]. Cyst diameters varied greatly as a function of their localization along the bronchiolar tree and the stage of the lesions. Accordingly, bullous defects develop from the destruction of distal respiratory bronchioles, particularly alveolar ducts, likely due to their thin anatomical architecture [25]. In addition, stretch emphysema of alveoli adjacent to CD1a$^+$-LC lesions or subpleural blebs could participate in the cystic appearance of PLCH lesions. All these features were observed in our biopsied patients. It is accepted that such cysts in adult PLCH result from progressive destruction of the bronchiole and the downstream airways. Subpleural cysts with mixed fibrotic and cellular lesions may originate from peribronchiolar cysts, bronchioloectasia or even from cavitation of subpleural LC aggregates, as shown in Fig. 1D.

The bronchiolar breakdown, highlighted by the keratin immunolabeling and attributed to CD1a$^+$-LC infiltration very early during postnatal life, challenges the recognized relationship of adult-PLCH pathogenesis with active smoking [4,5]. Indeed, herein, all 7 patients ≥14 years were active smokers at the time of biopsy and 5 had the clinical-radiological-histopathological pattern of adult PLCH. However, for 4 of them, disease onset preceded the lung biopsy from 3.5 to 12 years. Importantly, the microscopic analyses of those biopsies from the 6 young smokers did not demonstrate any of the usual smoking-related histological changes of adult PLCH (ie, respiratory bronchiolitis, emphysema, desquamative interstitial pneumonia-like reaction), probably because these adolescents' cumulative tobacco consumption remained low. No information related to passive smoking could be obtained for the other patients. Therefore, multiple lines of evidence provided by our study suggest that tobacco does not play a key role in the pathophysiology of all childhood PLCHs. Consequently, other inducers must be considered in children. In 1993, Haque and Mancuso reported proliferations of dendritic/Langerhans cells in the bronchioles of sudden infant death syndrome victims, suggesting a consequence of exposure to environmental antigens [26]. Hence, environmental factors or virus infections, frequent in infants, might trigger bronchiolar cell secretion of cytokines/growth factors (eg, granulocyte-macrophage colony-stimulating factor) and peribronchiolar CD1a$^+$-LC recruitment [27], a known major pathogenetic mechanism of LCH [28-30].

Despite strong general similarities with adult-PLCH lesions across children's ages, some significant distinctive patterns were discerned, but may have been under-evaluated because younger PLCH patients were biopsied less often. As previously described in 7 children [31], pulmonary parenchyma of

the costophrenic angles on CT scans was involved in all the children ≤13.5 years, unlike adult PLCH, which characteristically spares this part of the lung. That finding might suggest that deposition of potential airborne triggers varies according to bronchial maturation until puberty, a hypothesis consistent with the greatest pulmonary particle-deposition fraction in infants, then decreasing with age [32].

Unusual CD1a$^+$-LC-clustering patterns were observed in this series: large nodules in 2 patients or interstitial pneumonitis in a third. Extensive sheets of CD1a$^+$ LCs were observed in the biopsy of 2 of 7 ≤6-year-old children: a 3-month-old girl and a 2-year-old boy with RO$^+$ multiorgan disease. CT scan showed alveolar condensation. In a 16-year-old smoker girl with RO$^-$ disease (patient 15), we observed an interstitial and alveolar spread of CD1a$^+$ LCs with maintained alveolar architecture evocative of CD1a$^+$-LC interstitial pneumonitis. In that patient, diffuse ground-glass opacities were observed on CT scan. In a review of 59 patients, from the pediatric LCH series, alveolar condensations and ground-glass opacities, respectively, were observed in 24% and 17% of PLCHs (Valeria De la Valle et al personal communication; manuscript submitted). These unusual childhood-PLCH histological patterns suggest the possibility of dissemination throughout the lung parenchyma via circulating CD1a$^+$ LCs [33]. Moreover, the infiltrative pattern evocative of CD1a$^+$-LC interstitial pneumonitis is particularly unusual in PLCH, although rare LCs have been described in fibrotic interstitial diseases [34]. Indeed, the multiorgan diffusion observed in that patient suggests a possible hematogenous or extrapulmonary origin resulting in interstitial LC infiltration of alveolar walls. It must be emphasized that, herein, *BRAF*^{V600E} mutation was detected in these 3 patients with unusually extensive lesions. The percentage of *BRAF*^{V600E} mutations in the biopsy cohort (33%) was lower than that of the no-lung-biopsy group (64%). That finding can be explained by a sampling bias because of a low number of tests or by biopsy-cohort patients being significantly older. However, the overall *BRAF*^{V600E} rate (26/47; 55%) is in line with the previously published results [2].

In conclusion, the overall histopathology of most childhood PLCHs, regardless of age, mostly resembled that already described for adult disease. That observation raises the possibility, particularly for very young patients, of triggers other than tobacco smoke for bronchiolar CD1a$^+$-LC recruitment. A minority of our childhood PLCHs carrying the *BRAF*^{V600E} mutation exhibited unusually extensive interstitial CD1a$^+$-LC infiltration.

Acknowledgments

We are grateful to S. Boudjemaa (Pathology Department, APHP, Armand-Trousseau Hospital, Paris, France) and Z. Helias-Rodzewicz (APHP, Ambroise-Paré Hospital, Boulogne-Billancourt, France) for technical help, to F. Plénat (Pathology Department, Brabois Hôpital, Nancy, France) for his contribution, and to J. Jacobson (Paris, France) for editorial assistance. The study received a financial support from the patients'associations : Association Histiocytose France and RMHE (Recherche Maladies Hématologiques de l'Enfant).

References

[1] Collin M, Bigley V, McClain KL, et al. Cell(s) of origin of Langerhans cell Histiocytosis. Hematol Oncol Clin North Am 2015;29:825-38.
[2] Heritier S, Emile JF, Barkaoui MA, et al. BRAF mutation correlates with high-risk Langerhans cell Histiocytosis and increased resistance to first-line therapy. J Clin Oncol 2016;34:3023-30.
[3] Badalian-Very G, Vergilio JA, Degar BA, et al. Recurrent BRAF mutations in Langerhans cell histiocytosis. Blood 2010;116:1919-23.
[4] Tazi A, Jereon T, Hiltermann N, et al. Adult lung histiocytosis. In: Weitzman S, Egeler M, editors. Histiocytic Disorders of Children and Adults. Cambridge Press University; 2005. p. 187-207.
[5] Vassallo R, Harari S, Tazi A. Current understanding and management of pulmonary Langerhans cell histiocytosis. Thorax 2017;72:937-45.
[6] Donadieu J, Chalard F, Jeziorski E. Medical management of langerhans cell histiocytosis from diagnosis to treatment. Expert Opin Pharmacother 2012;13:1309-22.
[7] Basset F, Corrin B, Spencer H, et al. Pulmonary histiocytosis X. Am Rev Respir Dis 1978;118:811-20.
[8] Nezelof C, Frileux-Herbet F, Cronier-Sachot J. Disseminated histiocytosis X: analysis of prognostic factors based on a retrospective study of 50 cases. Cancer 1979;44:1824-38.
[9] Travis WD, Borok Z, Roum JH, et al. Pulmonary Langerhans cell granulomatosis (histiocytosis X). A clinicopathologic study of 48 cases. Am J Surg Pathol 1993;17:971-86.
[10] Colby TV, Lombard C. Histiocytosis X in the lung. Hum Pathol 1983; 14:847-56.
[11] Friedman PJ, Liebow AA, Sokoloff J. Eosinophilic granuloma of lung. Clinical aspects of primary histiocytosis in the adult. Medicine (Baltimore) 1981;60:385-96.
[12] Rigaud C, Barkaoui MA, Thomas C, et al. Langerhans cell histiocytosis: therapeutic strategy and outcome in a 30-year nationwide cohort of 1478 patients under 18 years of age. Br J Haematol 2016;174:887-98.
[13] Ronceray L, Potschger U, Janka G, et al. Pulmonary involvement in pediatric-onset multisystem Langerhans cell histiocytosis: effect on course and outcome. J Pediatr 2012;161:129-33.
[14] Haupt R, Minkov M, Astigarraga I, et al. Langerhans cell histiocytosis (LCH): guidelines for diagnosis, clinical work-up, and treatment for patients till the age of 18 years. Pediatr Blood Cancer 2013;60:175-84.
[15] Donadieu J, Piguet C, Bernard F, et al. A new clinical score for disease activity in Langerhans cell histiocytosis. Pediatr Blood Cancer 2004;43: 770-6.
[16] Tazi A, Marc K, Dominique S, et al. Serial computed tomography and lung function testing in pulmonary Langerhans' cell histiocytosis. Eur Respir J 2012;40:905-12.
[17] Galambrun C, Garaix F, Ughetto F, et al. Cladribine-related immunosuppression may have fostered graft-versus-host disease after lung transplant for pulmonary Langerhans cell histiocytosis. Pediatr Blood Cancer 2019; 66(1):e27477.
[18] Aftimos S, Nassar V, Najjar S. Primary pulmonary histiocytosis in an infant. Am J Dis Child 1974;128:851-2.
[19] Chatkin JM, Bastos JC, Stein RT, et al. Sole pulmonary involvement by Langerhans' cell histiocytosis in a child. Eur Respir J 1993;6:1226-8.
[20] Dejima H, Morita S, Takahashi Y, et al. A case of invasive Langerhans cell histiocytosis localizing only in the lung and diagnosed as pneumothorax in an adolescent female. Int J Clin Exp Pathol 2015;8: 3354-7.
[21] Knutsen AP, Goodman GM. A 13-month-old child with chronic diarrhea, weight loss, and tachypnea. Ann Allergy 1993;71:352-6.

[22] Nakhla H, Jumbelic MI. Sudden death of a patient with pulmonary Langerhans cell histiocytosis. Arch Pathol Lab Med 2005; 129:798-9.
[23] Aydin GB, Kibar E, Han U, et al. Pulmonary Langerhans cell histiocytosis in an infant: can passive smoking accelerate the disease progress? Pediatr Pulmonol 2007;42:565-7.
[24] Bois MC, May AM, Vassallo R, et al. Morphometric study of pulmonary arterial changes in pulmonary Langerhans cell Histiocytosis. Arch Pathol Lab Med 2018;142:929-37.
[25] Kambouchner M, Basset F, Marchal J, et al. Three-dimensional characterization of pathologic lesions in pulmonary langerhans cell histiocytosis. Am J Respir Crit Care Med 2002;166:1483-90.
[26] Haque AK, Mancuso MG. Proliferation of dendritic cells in the bronchioles of sudden infant death syndrome victims. Mod Pathol 1993;6: 360-70.
[27] Tazi A, Bouchonnet F, Grandsaigne M, et al. Evidence that granulocyte macrophage-colony-stimulating factor regulates the distribution and differentiated state of dendritic cells/Langerhans cells in human lung and lung cancers. J Clin Invest 1993;91:566-76.
[28] Emile JF, Tartour E, Brugieres L, et al. Detection of GM-CSF in the sera of children with Langerhans' cell histiocytosis. Pediatr Allergy Immunol 1994;5:162-3.
[29] Emile JF, Fraitag S, Leborgne M, et al. In situ expression of activation markers by Langerhans' cells containing GM-CSF. Adv Exp Med Biol 1995;378:101-3.
[30] Tazi A, Bonay M, Bergeron A, et al. Role of granulocyte-macrophage colony stimulating factor (GM-CSF) in the pathogenesis of adult pulmonary histiocytosis. Thorax 1996;51:611-4.
[31] Seely JM, Salahudeen Sr S, Cadaval-Goncalves AT, et al. Pulmonary Langerhans cell histiocytosis: a comparative study of computed tomography in children and adults. J Thorac Imaging 2012;27:65-70.
[32] Asgharian B, Menache MG, Miller FJ. Modeling age-related particle deposition in humans. J Aerosol Med 2004;17:213-24.
[33] Zhang L, Pacheco-Rodriguez G, Steagall WK, et al. BRAF and NRAS mutations in circulating Langerhans-like CD1a(+) cells in a patient with pulmonary Langerhans' cell histiocytosis. Eur Respir J 2017;50. pii: 1700521.
[34] Kawanami O, Basset F, Ferrans VJ, et al. Pulmonary Langerhans' cells in patients with fibrotic lung disorders. Lab Investig 1981;44:227-33.